Prevalence of Fundus Tessellation and Its Screening Based on Artificial Intelligence in Chinese Children: the Nanjing Eye Study

Dan Huang · Yingxiao Qian · Qi Yan · Saiguang Ling ·

Zhou Dong · Xin Ke · Haohai Tong · Tengfei Long · Rui Li ·

Hu Liu · Hui Zhu 🔟

ABSTRACT

Introduction: To investigate the prevalence of fundus tessellation (FT), and the threshold for screening FT using an artificial intelligence (AI) technology in Chinese children.
Methods: The Nanjing Eye Study was a population-based cohort study conducted in children born between September 2011 and August 2012 in Yuhuatai District of Nanjing. The data presented in this paper were obtained in 2019, when these children were 7 years old and underwent 45° non-mydriatic fundus photography. FT in whole fundus, macular area, and peripapillary area was manually recognized from fundus photographs and classified into three grades. Fundus tessellation density (FTD) in these areas was obtained by calculating the average exposed choroid area per unit area using artificial intelligence (AI) technology based on fundus photographs. The threshold for screening FT using FTD was determined using receiver operating characteristic (ROC) curve analysis.
Results: Among 1062 enrolled children (mean [± standard deviation] spherical equivalent: − 0.28 ± 0.70 D), the prevalence of FT was 42.18% in the whole fundus (grade 1: 36.53%; grade 2: 5.08%; grade 3: 0.56%), 45.57% in macular area (grade 1: 43.5%; grade 2: 1.60%; grade 3: 0.50%), and 49.72% in peripapillary area (grade 1: 44.44%; grade 2: 4.43%; grade 3: 0.85%), respectively. The threshold value of FTD for screening severe FT (grade ≥ 2) was

D. Huang · Y. Qian · Q. Yan · R. Li · H. Liu (✉) ·
H. Zhu (✉)
Department of Ophthalmology, The First Affiliated Hospital–Nanjing Medical University, No. 300 Guangzhou Road, Gulou District, Nanjing 210029, Jiangsu, China
e-mail: liuhu@njmu.edu.cn

H. Zhu
e-mail: zhny1125@njmu.edu.cn

S. Ling · Z. Dong · X. Ke
EVision Technology (Beijing) Co. Ltd., Shangdixinxi Road No.26, Haidian District, Beijing, China

H. Tong
Eye Center, The Second Affiliated Hospital, Zhejiang University School of Medicine, Jiefang Road No.88, Shangcheng District, Hangzhou, Zhejiang, China

T. Long
Aerospace Information Research Institute, Chinese Academy of Sciences (CAS), Dengzhuang South Road No. 9, Haidian District, Beijing, China

0.049 (area under curve [AUC] 0.985; sensitivity 98.3%; specificity 92.3%) in the whole fundus, 0.069 (AUC 0.987; sensitivity 95.5%; specificity 96.2%) in the macular area, and 0.094 (AUC 0.980; sensitivity 94.6%; specificity 94.2%) in the peripapillary area, respectively.

Conclusion: Fundus tessellation affected approximately 40 in 100 children aged 7 years in China, indicating the importance and necessity of early FT screening. The threshold values of FTD provided by this study had high accuracy for detecting severe FT and might be applied for rapid screening.

Key Summary Points

Why carry out this study?

Fundus tessellation (FT) is the earliest sign in the natural course of myopic maculopathy, and it is usually assessed and graded manually based on fundus photographs. However, little is known about its prevalence in 7-year-old Chinese children and how to screen it accurately and rapidly using artificial intelligence (AI) technology.

This study aimed to investigate the prevalence of FT, and the threshold for screening FT using AI technology in Chinese children.

What was learned from the study?

In this population-based study, FT affected approximately 40% Chinese children aged 7 years. The threshold values of fundus tessellated density (FTD), a quantitative index of FT obtained by AI technology, were determined by receiver operating characteristic curve analysis and verified to have high accuracy for detecting severe FT.

The high prevalence of FT in 7-year-old children indicates the importance and necessity of early FT screening, and the FTD thresholds provided in this study might be applied for rapid screening in the future.

INTRODUCTION

Myopia is a common cause of vision loss, and it is estimated that by 2050 there will be 49.8% of the world population with myopia and 9.8% with high myopia [1]. Myopic maculopathy is the most common myopic fundus lesion, and also the main cause of irreversible myopic visual impairment [2–4]. Fundus tessellation (FT), defined as the visibility of choroidal vessels at the posterior fundus pole, is the earliest sign in the natural course of myopic maculopathy and has close association with longer axial length, higher myopic refraction, and better best-corrected visual acuity (BCVA) [5, 6]. School-based studies found that the prevalence of FT was 48.1% among children aged 9–16 years with various refractive status and 52.4% among children aged 9–12 years with low myopia [6, 7]. Therefore, screening of FT in children is necessary and beneficial for timely prevention and management of pathological myopic lesions.

FT is usually assessed and graded by ophthalmologists subjectively based on fundus photographs. This manual method is time-consuming and has a lack of repeatability, which limits its use in FT screening. Yoshihara et al. introduced three objective indexes of FT by calculating the average intensity of red, green, and blue pixels within a circular area of 250-pixel diameter between the fovea and the optic disc using the ImageJ software [8]. However, this method is easily affected by fundus color and cannot represent the degree of FT outside the circular area. Pan et al. developed a deep learning-based system using Inception V3 and ResNet-50 models to categorize fundus images into three classes: normal, macular degeneration, and FT, which is a qualitative method to check whether FT is present [9]. Recently, a new quantitative method was proposed, which is based on artificial intelligence (AI) image processing technology to first extract the exposed choroid from the fundus and then calculate the average exposed choroid area per unit area of the fundus; this method is named fundus tessellated density (FTD) [10, 11]. It has been reported that AI-based imaging processing could improve the accuracy of FT diagnosis in

young adults [11]. In one study that applied machine learning methods employing gender, age, and FTD as major factors, the correct classification rate of FT severity was reported to be 77.12–81.28% among the elderly [12]. FTD may help to quickly identify and classify FT in screening setting.

In this study, we aimed to investigate the prevalence of FT and evaluate the threshold and accuracy of FTD obtained by AI technology for FT screening in 7-year-old primary school children.

METHODS

Study Population

The Nanjing Eye Study (NES) is an ongoing population-based cohort study in eastern China, with the aim to investigate the occurrence and development of ocular diseases in children longitudinally. The details of NES have been reported previously [13, 14]. In brief, all children born in Yuhuatai District, Nanjing, China between September 2011 and August 2012 and entering kindergartens in Yuhuatai District were invited to participate in the NES for comprehensive eye examinations annually, beginning in 2015. This study is part of the NES and the data presented here were obtained in 2019 when these children were 7 years old. Children who completed comprehensive examinations were included in the analysis, and those with incomplete examinations data, history of intraocular surgery, chorioretinal or vitreoretinal abnormalities except for FT, systemic diseases, or low-quality fundus images were excluded from this study.

The study was approved by the Ethics Committee of the First Affiliated Hospital with Nanjing Medical University and followed the tenets of the Declaration of Helsinki. Written informed consent was obtained from the parents or legal guardians of all children, and oral assent was obtained from all participants immediately before the examination.

Eye and Anthropometric Examinations

Comprehensive examinations, including BCVA, ocular surface, anterior segment, posterior segment, refraction, ocular alignment and motility, ocular biometric parameters, and intraocular pressure, were performed in the school during school breaks by a trained team composed of ophthalmologists and optometrists.

Noncycloplegic refraction was performed using an autorefractor (model RF10; Canon Inc., Tokyo, Japan) and retinoscopy, and spherical equivalent (SE) was calculated as sphere plus half of cylinder. Axial length (AL) and corneal radius of curvature (CR) were measured with the IOLMaster-500 (Carl Zeiss Meditec AG, Jena, Germany). A non-mydriatic fundus camera (model CR-2; Canon Inc.) was used to capture 45° fundus photographs centered on macula. The camera was operated by trained and experienced examiners in a dim room to ensure that the pupil diameter was > 4 mm and the acquired fundus images were in focus. Height and weight of each participating child were measured without shoes and heavy clothing, and body mass index was calculated as weight in kilograms divided by the square of height in meters (kg/m^2).

Manual Grading of FT

The quality of fundus images was assessed according to the following four criteria:

(1) Focus: the image is focused exactly on the retina and the retinal features can be clearly identified.
(2) Illumination: the image is properly exposed, neither overexposed (the image is low in contrast and has white tones) nor underexposed (the image is low in brightness and difficult to identify retinal features).
(3) Image field: the center of the image is located between the macula and the optic disc, and both of the optic disc and macula are at least one optic disc diameter away from the edge of the image.

(4)   Artifacts: there are no artifacts in the image that would interfere with the recognition of fundus features, such as dust spot, arc defect, fingerprint, camera reflex, eyelash image, among others.

Fundus images that did not meet the above criteria were identified as low-quality images and excluded from analysis.

The whole fundus, the macular area (a circle with a diameter of 6 mm centering on fovea), and the peripapillary area (a circle with a diameter of 4 mm centering on the optic disc) were assessed separately using 45° fundus photographs centered on the macula. FT was graded according to the study of Yan and his colleagues [5], with grade 0 referring to "no visibility of the large choroidal vessels outside the region of the parapapillary beta zone"; grade 1 referring to "slight visibility"; grade 2 referring to "moderate visibility"; and grade 3 referring to "marked visibility". During FT grading, the contrast, brightness, background pigmentation, and quality of images were taken into account, and standard photographs were used to recalibrate subjective assessments. Two trained ophthalmologists (QYX and YQ) independently graded the FT of all images in a blinded manner; in the case of disagreement, a senior ophthalmologist (HL) was asked to make the decision. The fluctuations in measurements among the two ophthalmologists (QYX and YQ) were used to test inter-observer variability. To determine intra-observer variability, 100 images of 100 children were randomly selected and read twice by an ophthalmologist (QYX) in a blinded manner at an interval of 2 weeks. The intra-observer and inter-observer kappa values were > 0.80.

Extraction of FTD by AI Technology

The signal strength of image data was evaluated by a fundus image quality assessment system, which consists of evaluations of exposure level and clarity of fundus images [15]. More technical details were described in supplementary materials. All fundus images that passed the quality control in both the image acquisition and manual FT grading processes had also passed the signal strength evaluation.

We then used AI image processing technology based on deep learning, as reported in previous studies [10–12], to extract exposed choroid images from fundus images and obtain the average exposed choroid area per unit area of the fundus, named the FTD. Briefly, this process consisted of preprocessing, sample labeling, segmentation by deep learning and computer vision methods, and FTD computation.

Firstly, fundus images were preprocessed in four steps, namely, establishment of a region of interest (ROI), denoising, normalization, and enhancement, to improve the differences between the internal features of each image and to reduce the differences between images [16]. Secondly, sample labeling was performed through channel calculation, as well as manual modification and review. Thirdly, exposed choroids and atrophic arcs were extracted by a semantic segmentation network model based on deep learning. Optic disc and macula were automatically recognized based on a visual attention mechanism to locate the optic disc center and macular fovea [15]. Finally, on the basis of the results of fundus feature recognition and segmentation, FTD was calculated for the whole fundus, for the macular area (a circle with a diameter of 6 mm centered on the fovea), and for the peripapillary area (a circle with a diameter of 4 mm centered on the optic disc) (as shown in Fig. 1). The technical aspects are described in detail in the text of the Electronic Supplementary Material (ESM).

Statistical Analysis

Data analysis was performed using the IBM Statistical Package for the Social Sciences program statistical package V13.0 (SPSS, IBM Corp., Armonk, NY, USA). Data on the right eye were included in this analysis. Analysis of variance (ANOVA) was performed to compare FTD, SE, AL, CR, and AL/CR among the different FT grades. We created receiver operating characteristic (ROC) curves and calculated the area under curve (AUC) and cut-off values of FTD. The accuracy of the cut-off values for detecting different FT grades was evaluated by sensitivity,
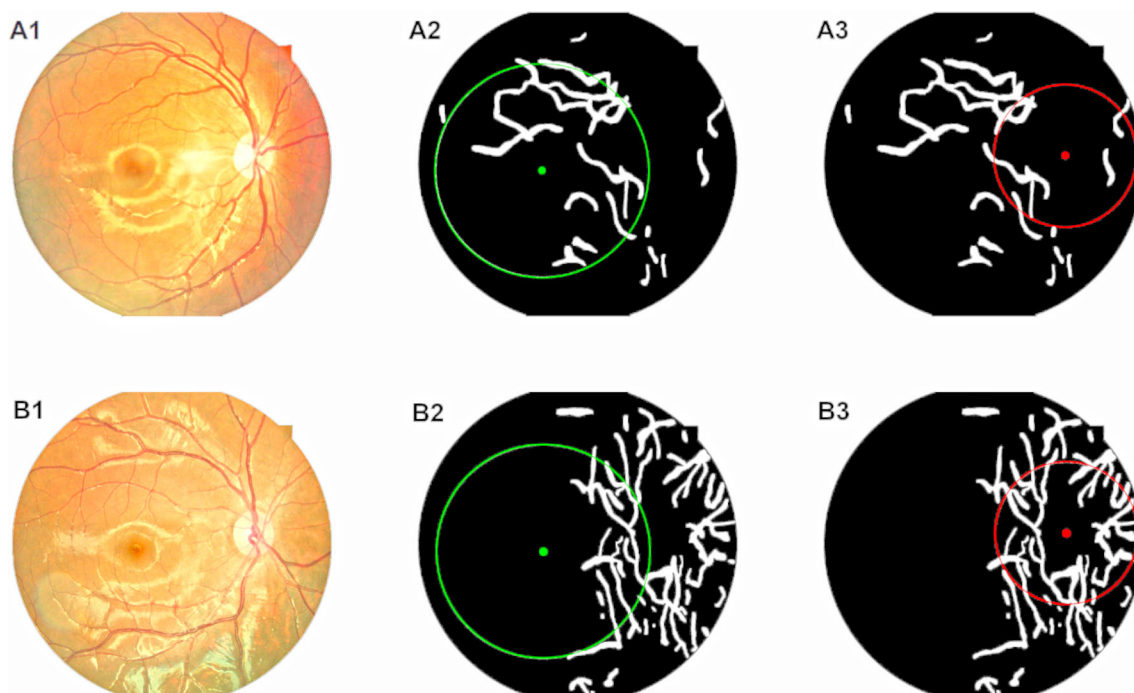
Fig. 1 Quantification of fundus tessellated density by artificial intelligence technology. **a** An eye in the macular distributed group, **b** an eye in the peripapillary distributed group. **a1**, **b1** original image, **a2**, **b2** fundus tessellation in the macular area (circle of 6-mm diameter centered on the fovea; shown in figure as a green circle), **a3**, **b3** fundus tessellation in the peripapillary area (circle of 4-mm diameter centered on the optic disc; shown in figure as a red circle)

specificity, and Youden index. All *P* values were two-sided and considered to be statistically significant at $P < 0.05$. The 95% confidence intervals (CIs) were determined. Continuous variables were described as mean ± standard deviation (SD), while frequency count and percentage were used for the categorical measures. Myopia was defined as SE ≤ -0.50 D; emmetropia as SE > -0.50 D and $\leq +1.00$ D; hyperopia as SE $> +1.00$ D.

RESULTS

Of the 1565 eligible children, 1090 were recruited and completed comprehensive examinations (69.65%); of these 1090 children, 28 were excluded, including nine children with systemic diseases and 19 children with low-quality fundus images. Therefore, a total of 1062 children were included in the analysis. Between the 1062 children included in the analysis and the 503 children excluded, there

was no statistical difference in gender (boys: 51.88% vs. 56.97%; $P = 0.06$) and only a small difference in age (mean ± SD: 7.38 ± 0.29 vs. 7.32 ± 0.30; $P = 0.001$). Table 1 lists the characteristics of the 1062 children, including the mean (± SD) SE of -0.28 ± 0.70 D (range -3.88 to 4.50 D), mean AL of 22.97 ± 0.77 mm (range 19.25–26.22 mm), and mean AL/CR ratio of 2.94 ± 0.08 (range 2.62–3.24). The majority of children were emmetropic (72.89%, 774/1062), 25.42% were myopic (270/1062), and a small proportion were hyperopic (1.69%, 18/1062). Children with myopia found to have more severe FT and higher FTD than those with hyperopia (all $P < 0.05$; ESM Tables 1 and 2).

As shown in Table 2, the overall prevalence of FT in whole fundus was 42.18% (95% CI 39.21–45.16), with 36.53% prevalence (95% CI 33.63–39.44) of grade 1 FT, 5.08% prevalence (95% CI 3.76–6.41) of grade 2 FT, and 0.56% prevalence (95% CI 0.11–1.02) of grade 3 FT. The overall prevalence of FT in the macular area

Table 1 Demographic information on the right eyes of eligible children

Characteristics	Mean	Standard deviation	Range
Systemic parameters			
Age (years)	7.38	0.29	6.83–7.83
Sex (boy:girl)	551:511		NA
Height (cm)	128.73	6.50	94.50–167.00
Weight (kg)	27.25	5.71	16.40–58.00
BMI (kg/m^2)	16.37	2.69	9.22–38.41
Ophthalmologic parameters			
Intraocular pressure (mmHg)	18.53	2.47	10.00–26.00
BCVA (LogMAR)	0.01	0.04	− 0.10–0.30
Axial length (mm)	22.97	0.77	19.25–26.22
AL/CR atio	2.94	0.08	2.62–3.24
Corneal radius of curvature (mm)	7.80	0.24	7.02–8.76
Spherical equivalent (D)	− 0.28	0.70	− 3.88–4.50
FTD			
Whole fundus image	0.023	0.025	0.000–0.181
Macular area (6-mm diameter)	0.020	0.025	0.000–0.163
Peripapillary area (4-mm diameter)	0.035	0.046	0.000–0.350

AL/CR Axial length/corneal radius of curvature ratio, *BCVA* best corrected visual acuity, *BMI* body mass index, *FTD*, fundus tessellation density, *NA*, not applicable;

was 45.57% (95% CI 42.57–48.57), with 43.5% prevalence (95% CI 40.52–46.49) of grade 1 FT, 1.60% prevalence of (95% CI 0.84–2.36) of grade 2 FT, and 0.50% prevalence (95% CI 0.10–0.90] of grade 3 FT. The overall prevalence of FT in the peripapillary area was 49.72% (95% CI 46.71–52.73), with 44.44% prevalence (95% CI 41.45–47.44)) of grade 1 FT, 4.43% prevalence (95% CI 3.19–5.66) of grade 2 FT, and 0.85% prevalence (95% CI 0.30–1.40) of grade 3 FT. In addition, five of the nine children excluded from the analysis due to systemic diseases were identified as having FT (3 with grade 1 FT and 2 with grade 2 FT).

FTD, AL, and CR in the whole fundus, macular area, and peripapillary area increased significantly with increasing grade of FT in these areas (all $P < 0.05$; Table 2, Fig. 2). There was a borderline significant difference in SE among

the different grades of FT in the macular area ($P = 0.029$), but no significant difference in other areas. AL/CR was also not significantly different among the different grades of FT in all areas.

The ROC curve analysis showed that for FT in the whole fundus, the cut-off values of FTD were 0.016 in grade $\geq$ 1 (AUC 0.949, sensitivity 89.3%, specificity 86.8%), 0.049 in grade $\geq$ 2 (AUC 0.985, sensitivity 98.3%, specificity 92.3%), and 0.060 in grade 3 (AUC 0.984, sensitivity 100.0%, specificity 92.1%), respectively (Table 3; Fig. 3a). For FT in the macular area, the cut-off values of FTD were 0.013 in grade $\geq$ 1 (AUC 0.890, sensitivity 77.3%, specificity 84.8%), 0.069 in grade $\geq$ 2 (AUC 0.987, sensitivity 95.5%, specificity 96.2%), and 0.091 in grade 3 (AUC 0.994, sensitivity 100.0%, specificity 97.7%), respectively (Table 3; Fig. 3b). For

Table 2 Prevalence of fundus tessellation, and differences in fundus tessellation density and ocular biometric parameters between the different fundus tessellation groups

Fundus tessellation groups[a]	Number of children	Prevalence, % (95% CI)	Mean FTD	FTD standard deviation	P^b	SE	P^b	AL/CR	P^b	AL	P^b	CR	P^b
Whole fundus image	1062	42.18 (39.21–45.16)	0.023	0.025	< 0.001		0.88		0.86		0.01		0.001
Grade 0	614	57.82 (54.84–60.79)	0.009	0.007		− 0.27 ± 0.66		2.94 ± 0.08		22.91 ± 0.75		7.79 ± 0.24	
Grade 1	388	36.53 (33.63–39.44)	0.035	0.017		− 0.30 ± 0.68		2.94 ± 0.08		23.02 ± 0.80		7.83 ± 0.25	
Grade 2	54	5.08 (3.76–6.41)	0.089	0.027		− 0.25 ± 0.75		2.95 ± 0.06		23.14 ± 0.64		7.85 ± 0.23	
Grade 3	6	0.56 (0.11–1.02)	0.130	0.040		− 0.25 ± 0.29		2.93 ± 0.05		23.66 ± 0.42		8.06 ± 0.14	
Macular area (6-mm diameter)	1062	45.57 (42.57–48.57)	0.020	0.025	< 0.001		0.03		0.10		< 0.001		0.02
Grade 0	578	54.43 (51.43–57.43)	0.007	0.009		− 0.25 ± 0.69		2.94 ± 0.08		22.88 ± 0.76		7.78 ± 0.24	
Grade 1	462	43.5 (40.52–46.49)	0.032	0.024		− 0.32 ± 0.64		2.95 ± 0.08		23.05 ± 0.77		7.83 ± 0.25	
Grade 2	17	1.60 (0.84–2.36)	0.103	0.026		− 0.25 ± 0.75		2.95 ± 0.06		23.24 ± 0.66		7.83 ± 0.23	
Grade 3	5	0.50 (0.10–0.90)	0.131	0.027		− 0.25 ± 0.29		2.93 ± 0.05		23.78 ± 0.66		7.91 ± 0.14	
Peripapillary area (4-mm diameter)	1062	49.72 (46.71–52.73)	0.035	0.046	< 0.001		0.72		0.60		0.00		< 0.001
Grade 0	534	50.28 (47.27–53.29)	0.009	0.014		− 0.27 ± 0.71		2.95 ± 0.08		22.90 ± 0.77		7.78 ± 0.24	
Grade 1	472	44.44 (41.45–47.44)	0.051	0.036		− 0.29 ± 0.62		2.94 ± 0.08		23.02 ± 0.76		7.83 ± 0.24	
Grade 2	47	4.43 (3.19–5.66)	0.145	0.045		− 0.28 ± 0.74		2.94 ± 0.07		23.12 ± 0.68		7.87 ± 0.25	
Grade 3	9	0.85 (0.30–1.40)	0.220	0.084		− 0.53 ± 0.68		2.98 ± 0.07		23.71 ± 0.52		7.95 ± 0.14	

Vales for SE, AL/CR, AL, and CR are given as the mean ± standard deviation (SD)

AL Axial length (mm),AL/CR axial length/corneal curvature ratio, CI confidence interval, CR, corneal radius of curvature (mm), FTD fundus tessellation density, SE spherical equivalent (D)

[a]See section Manual Grading of FT for detailed description of the grades

[b]Analysis of variance (ANOVA) was performed to compare FTD, SE, AL/CR, AL, CR at different grades of severity. Statistical significance was set at $P < 0.05$
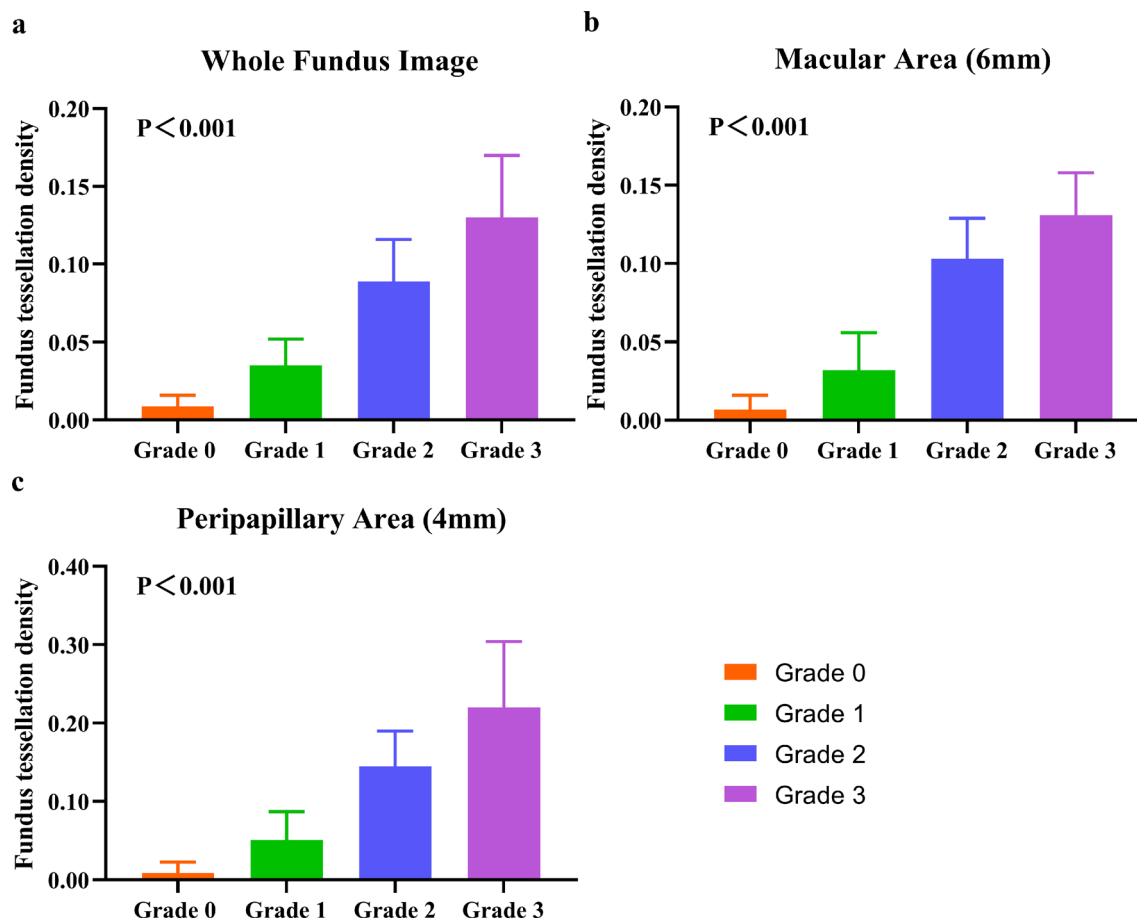
a

Whole Fundus Image

b

Macular Area (6mm)

c

Peripapillary Area (4mm)

- ■ Grade 0
- ■ Grade 1
- ■ Grade 2
- ■ Grade 3

Fig. 2 Fundus tessellation density (FTD) in the whole fundus (**a**), macular area (**b**), and peripapillary area (**c**). FTD in the macular area was measured in a circle with a diameter of 6 mm centering on the fovea); in the peripapillary area, FTD was measured in a circle with a diameter of 4 mm centering on the optic disc. Bars are the means and whiskers are the standard deviations. See section Manual Grading of FT for detailed description of the grades

FT in the peripapillary area, the cut-off values of FTD were 0.018 in grade ≥ 1 (AUC 0.917, sensitivity 85.2%, specificity 83.7%), 0.094 in grade ≥ 2 (AUC 0.980, sensitivity 0.946%, specificity 0.942%), and 0.118 in grade 3 (AUC 0.984, sensitivity 100.0%, specificity 94.3%), respectively (Table 3, Fig. 3c).

DISCUSSION

In this study of 7-year-old children who were predominantly emmetropic, the prevalence of FT in the whole fundus, macular area, and peripapillary area ranged from 42.18% to 49.72%. Moreover, severe FT (grade ≥ 2) was found among 5.64% children in the whole fundus, 2.10% children in the macular area, and 5.28% children in the peripapillary area, respectively. The cut-off values of FTD determined by the ROC curve analysis had good sensitivity (≥ 94.6%) and specificity (≥ 92.3%) for screening severe FT in the whole fundus, macular area, and peripapillary area. To our knowledge, this is the first attempt to screen FT using AI technology in children. The cut-off values of FTD found in this study might be helpful for rapid screening of severe FT in children.

Multiple studies in recent years have reported the prevalence of FT among different

Table 3 Accuracy of fundus tessellated density for assessing fundus tessellation

Fundus tessellation groups	Number of children	AUC	Sensitivity	Specificity	Youden index	Cut-off value
Whole fundus image						
≥ 1	448	0.949	0.893	0.868	0.761	0.016
≥ 2	60	0.985	0.983	0.923	0.906	0.049
3	6	0.984	1.000	0.921	0.921	0.060
Macular area (6-mm diameter)						
≥ 1	484	0.890	0.773	0.848	0.620	0.013
≥ 2	22	0.987	0.955	0.962	0.916	0.069
3	5	0.994	1.000	0.977	0.977	0.091
Peripapillary area (4-mm diameter)						
≥ 1	528	0.917	0.852	0.837	0.689	0.018
≥ 2	56	0.980	0.946	0.942	0.889	0.094
3	9	0.984	1.000	0.943	0.943	0.118

AUC Area under curve

populations with various refractive status (Table 4) [5–8, 10, 11, 17–21]. Although comparisons between these studies are limited by inconsistent grading and/or classification methods, the findings demonstrate that FT is a universal fundus sign in myopic people. In hospital-based studies using the ETDRS grid to grade the degree of FT, the prevalence of FT exceeded 90% in young individuals with moderate or high myopia [19, 20]. In our study among 7-year-old children who were mainly emmetropic, the prevalence of severe FT in the macular area was lower than that reported in a school-based study among junior students with low myopia using the same grading method as our study (2.1% vs. 5.45%); however, the prevalence of mild FT (grade 1) in the macular area in the present study was similar to that in the school-based study (43.5% vs. 42.66%) [6]. In addition, the prevalence of severe FT in both the whole fundus and peripapillary area was approximately 5% in our study. Furthermore, our study showed that mean AL became longer with increasing FT grade, although no or only borderline significant differences in SE and AL/ CR were found between different FT grades,

which might be caused by increased CR with higher FT grades. These findings imply that FT has become a common fundus change in 7-year-old children who are supposed to have a healthy fundus in general, possibly indicating that it is a portent of rapid AL growth and myopia development in these children. A previous longitudinal study showed that about 19% of eyes with FT progressed into more severe fundus lesions within 10 years of follow-up, including diffuse chorioretinal atrophy, lacquer crack, patchy atrophy, and macular atrophy [22]. Thus, it is reasonable to conduct FT screening in children to identify their potential risk of myopic fundus lesions, even though they are not myopic.

Sensitivity, specificity, and Youden index are widely used indicators for evaluating the accuracy of a screening method. In our study, the cut-off values of FTD exhibited increased sensitivity, specificity, and Youden index with increasing degree of FT from grade ≥ 1, grade ≥ 2, to grade 3 in all of the three areas (whole fundus, peripapillary area, and peripapillary area). For severe FT (grade ≥ 2), sensitivity and specificity had exceeded 0.9, and the Youden
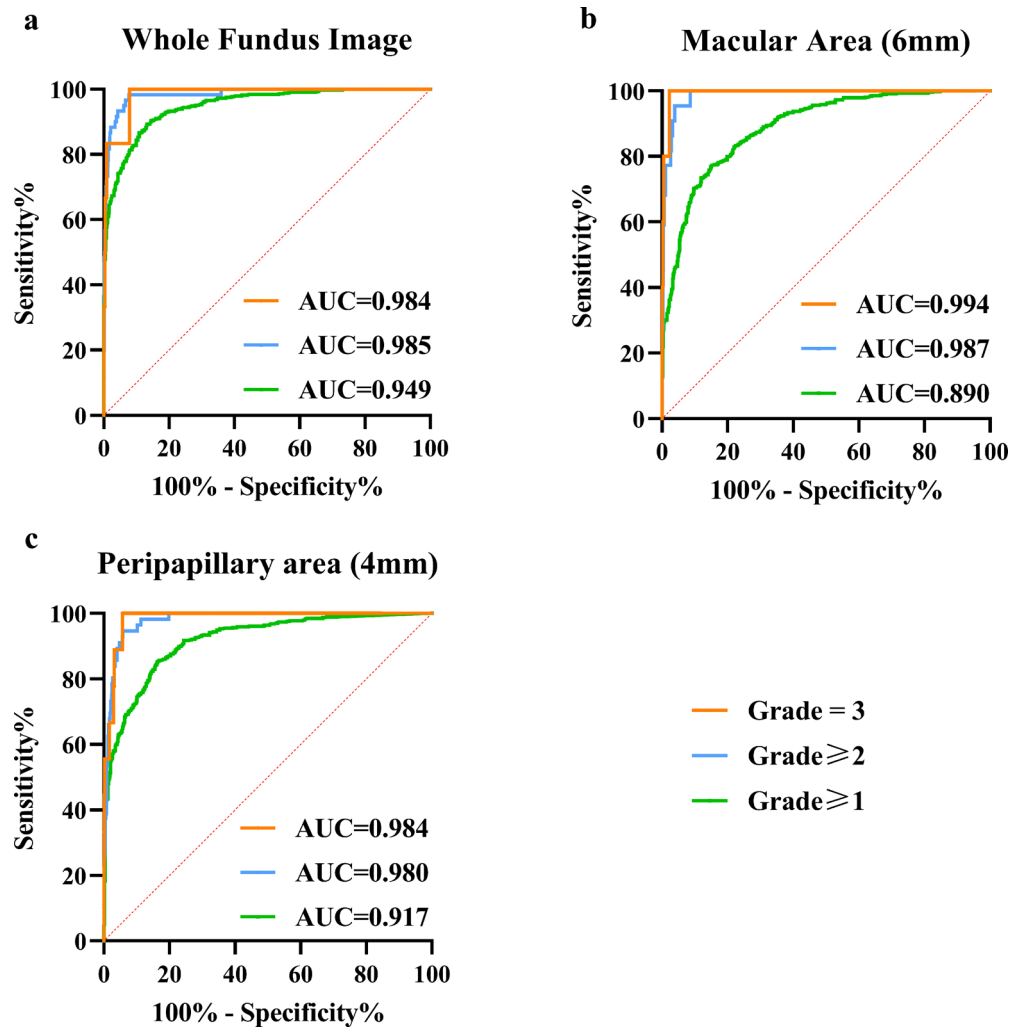
Fig. 3 Receiver operating characteristic curve analysis for fundus tessellation density detecting severe fundus tesselation (grade ≥ 2). **a** Whole fundus image, **b** macular area, **c** peripapillary area. *AUC* Area under the curve

index was > 0.8. For grade 3 FT, sensitivity even reached 1.0, and the Youden index was > 0.9. Given the higher prevalence of severe FT than that of grade 3 FT, the threshold values of FTD for detecting severe FT found by our study are more highly recommended in screening settings.

As mentioned in the Introduction, a previous study that used machine learning methods employing gender, age, and FTD as major factors to predict FT severity reported a good classification rate [12]. In addition, a deep learning-based system was developed to identify the presence of macular degeneration and FT in fundus photographs, with an accuracy up to

93.81% and 91.76% using the ResNet-50 and Inception V3 models, respectively [9]. Another deep learning system for screening myopic maculopathy based on fundus photographs was developed and obtained AUCs > 0.96 for different types of myopic maculopathy in the external-testing dataset [23]. Compared with these machine learning methods and deep learning systems, the method for screening FT based on FTD obtained by AI image processing technology used in our study is not only easier but also more available, as it can be achieved by installing software in a fundus camera, but it can also achieve quantitative results with high accuracy. As myopic fundus lesions more severe

Table 4 Prevalence and density of fundus tessellation in different studies

Study	Year	Location	Sample size (N)	Setting	Age, years, mean ± SD [range]	Refraction, D, mean ± SD [range]	Grading or classification methods	Fundus tessellation			
								Area	Prevalence (%)	Average grade (± SD)	FTD (mean ± SD)
Yoshihara et al. [8]	2014	Kagoshima, Japan	100	Hospital	25.8 ± 3.9 [22–39]	− 4.6 ± 3.3 [− 13.0 to 0.0]	Non/weakly/strongly tessellated group	Whole fundus	43	NA	NA
Yan et al. [5]	2015	Beijing, China	3442	Community	64.6 ± 9.8 [50–93]	− 0.20 ± 2.16 [− 22.00 to 15.00]	Visibility of the large choroidal vessels	Macular	NA	0.84 ± 0.79	NA
								Peripapillary	NA	1.01 ± 0.62	NA
Terasaki et al. [17]	2016	Kagoshima, Japan	126	Hospital	26.0 ± 4.1 [22–4])	− 4.71 ± 3.41 [− 14.25 to 4.50]	Curtin's classification[a]	Peripapillary	65.1	NA	NA
Yamashita et al. [21]	2018	Kumejima, Japan	1670	Community	53.6 ± 10.3 [40–88]	− 0.14 ± 1.62 [− 7.63 to 5.50]	Curtin's classification[b]	Whole Fundus	45.4	NA	NA
								Macular	7.1	NA	NA
								Peripapillary	22.9	NA	NA lePara>
Guo et al. [6]	2019	Beijing, China	1430	School	12.4 ± 0.5 [9– 16]	− 2.39 ± 2.17 [− 15.6 to 4.25]	Visibility of the large choroidal vessels	Macular	48.1	0.54 ± 0.61	NA
								Grade 1	42.66	NA	NA
								Grade 2 & 3	5.45	NA	NA
								Peripapillary	NA	0.86 ± 0.68	NA
Shao et al. [10]	2021	Beijing, China	3074	Community	64.1 ± 9.7 [50–93]	− 0.13 ± 1.96 [− 20.0 to 13.50]	NA	NA	NA	NA	0.14 ± 0.08
Cheng et al. [19]	2021	Shanghai, China	513	Hospital	13.5 ± 3.1 [4– 19]	− 8.34 ± 1.91 [− 14.375 to − 5.000]	ETDRS grid[c]	Macular	94.3	NA	NA
								Grade 1	18.5	NA	NA
								Grade 2	45.4	NA	NA
								Grade 3	30.4	NA	NA
Lyu et al. [20]	2021	Shanghai, China	796	Hospital	With FT: 19.86 ± 2.20 Without FT: 19.82 ± 2.66	With FT: − 2.94 ± 2.20 Without FT: − 4.32 ± 2.38	ETDRS grid[c]	Macular	90.2	NA	NA
								Grade 1	7.66	NA	NA
								Grade 2	27.64	NA	NA
								Grade 3	33.54	NA	NA
								Grade 4	21.36	NA	NA

Table 4 continued

Study	Year	Location	Sample size (N)	Setting	Age, years, mean ± SD [range]	Refraction, D, mean ± SD [range]	Grading or classification methods	Fundus tessellation			
								Area	Prevalence (%)	Average grade (± SD)	FTD (mean ± SD)
Gong et al. [7]	2022	Shanghai, China	1127	School	10.29 ± 0.60 [9–12]	− 1.44 ± 0.69 [− 3.00 to − 0.50]	ETDRS grid[c]	Macular	52.4	NA	NA
								Grade 1	38	NA	NA
								Grade 2	11.4	NA	NA
								Grade 3	3.1	NA	NA
Runkuan et al. [11]	2023	Shandong, China	1002	School	19.32 ± 1.11 [17–23]	− 4.55 ± 2.33	NA	Whole fundus	NA	NA	0.06 ± 0.06
								Macular	NA	NA	0.07 ± 0.09
This study	NA	Nanjing, China	1062	Population	7.38 ± 0.29 [6.83–7.83]	− 0.28 ± 0.70 [− 3.88 to 4.50]	Visibility of the large choroidal vessels[d]	*Whole fundus*	42.18	0.42 ± 0.62	0.02 ± 0.03
								Grade 1	36.53	NA	0.04 ± 0.02
								Grade 2	5.08	NA	0.09 ± 0.03
								Grade 3	0.56	NA	0.13 ± 0.04
								Macular	45.57	0.48 ± 0.56	0.02 ± 0.03
								Grade 1	43.5	NA	0.03 ± 0.02
								Grade 2	1.6	NA	0.10 ± 0.03
								Grade 3	0.5	NA	0.13 ± 0.03
								Peripapillary	49.72	0.56 ± 0.62	0.04 ± 0.05
								Grade 1	44.44	NA	0.05 ± 0.04
								Grade 2	4.43	NA	0.15 ± 0.05
								Grade 3	0.85	NA	0.22 ± 0.08

EDTRS Early Treatment of Diabetic Retinopathy Study, *FT* fundus tessellation, *FTD* fundus tessellation density, *NA* not mentioned, *SD* standard deviation

[a] Eight primary types based on Curtin's classification of the location of posterior staphyloma: no tessellation, temporal, infra-temporal, inferior, nasal, peripapillarly, whole, and unclassified tessellations

[b] Five primary types based on Curtin's classification of the location of posterior staphylomas: in the posterior pole, macular region, peripapillary, nasal, or inferior

[c] No involvement of the outer circle (grade 0, including eyes without tessellation); involvement of the outer circle (grade 1); involvement of the middle circle (grade 2); involvement of the inner circle without involving the fovea (grade 3); and involvement of the center fovea (grade 4)

[d] See section Manual Grading of FT for detailed description of the grades

than FT are infrequent in children and because FT is the earliest sign in the natural course of myopic maculopathy, the method provided in our study is suitable for fundus screening as well as for the prevention and control of myopia among children, especially in underdeveloped areas and medical institutions lacking ophthalmologists. Moreover, a telemedicine platform could be established based on this AI technology, further enhancing accessibility and affordability of FT screening. It is also important to note that the accuracy of the AI image processing technology can be affected by the quality of fundus images, thus quality control of fundus images should be considered during the application of this technology.

This study has two main advantages. Firstly, we reported the prevalence of FT in an age-specific population, which is important as FT is closely related to age [19, 22]. The age-specific setting is helpful to attenuate the effect of age on FT. In addition, children aged 7 years are mainly emmetropic and at the beginning of developing myopia; consequently, investigations in this age group may provide some information on the change in the fundus in the premyopic stage. Secondly, we applied an AI-based indicator, FTD, to explore rapid screening for FT in children, which has a high practical value. However, the study also has several limitations that must be considered. Firstly, the manual grading of FT based on color fundus photographs may be subject to subjective bias, especially in borderline cases. Nonetheless, the graders were well-trained ophthalmologists, and in cases of disagreement, a third, senior ophthalmologist made the final decision; this approach can reduce the bias as much as possible. Secondly, cycloplegic refraction was not available in this study due to its interference with children's subsequent learning, which might limit the assessment of the association between myopia and FT grade. However, we evaluated the difference in AL/CR between different FT grades as a supplementary study. Previous studies have demonstrated that AL/CR is a second choice to predict SE when cycloplegic refraction is difficult to perform in children [24, 25]. Also, a recent study assessed the association between refractive status under cycloplegia and fundus tessellation in 9- to 12-year-old school children with low myopia, and found no significant difference in cycloplegic SE between different FT grades, which is consistent with our findings, indicating that the influence of noncycloplegic refraction used in our study is acceptable [7]. Finally, there is a possibility that the cut-off values of FTD provided in our study may not be applicable to children of other ages and ethnicities. Further research is warranted to validate the accuracy of these cut-off values in other populations.

CONCLUSIONS

Fundus tessellation was found to be a common fundus change in 7-year-old children from eastern China who were mainly emmetropic, indicating the importance of FT screening. The threshold values of FTD based on AI image processing technology provided in this study had a high accuracy for detecting severe FT. This technology has the potential to be applied for rapid FT screening among children in the future.

ACKNOWLEDGEMENTS

Data Availability. The datasets generated during and/or analyzed during the current study are available from the corresponding author on reasonable request.

Ethical Approval. The study was approved by the Ethics Committee of the First Affiliated Hospital with Nanjing Medical University and followed the tenets of the Declaration of Helsinki (2017-SR-205). Written informed consent was obtained from the parents or legal guardians of all children, and oral assent was obtained from all participants right before examinations.

Conflict of Interest. No financial or non-financial benefits have been received or will be received from any party related directly or indirectly to the subject of this article. All authors confirm they have no conflicts of interest to declare.

REFERENCES

1. Holden BA, Fricke TR, Wilson DA, et al. Global prevalence of myopia and high myopia and temporal trends from 2000 through 2050. Ophthalmology. 2016;123(5):1036–42.

2. Xu L, Wang Y, Li Y, et al. Causes of blindness and visual impairment in urban and rural areas in Beijing: the Beijing Eye Study. Ophthalmology. 2006;113(7):1134.e1-11.

3. Hsu WM, Cheng CY, Liu JH, Tsai SY, Chou P. Prevalence and causes of visual impairment in an elderly chinese population in taiwan: the shihpai eye study. Ophthalmology. 2004;111(1):62–9.

4. Franco PJ, Suwezda A, Schlottmann P, et al. Analysis of visual disability in Buenos Aires, Argentina. Pathologic myopia is the leading cause in working age. Medicina (B Aires) 2021;81(5):735–41.

5. Yan YN, Wang YX, Xu L, et al. Fundus tessellation: prevalence and associated factors: the Beijing Eye Study 2011. Ophthalmology. 2015;122(9):1873–80.

6. Guo Y, Liu L, Zheng D, et al. Prevalence and associations of fundus tessellation among junior students from greater Beijing. Invest Ophthalmol Vis Sci. 2019;60(12):4033–40.

7. Gong W, Cheng T, Wang J, et al. Role of corneal radius of curvature in early identification of fundus tessellation in children with low myopia. Br J Ophthalmol 2022. https://doi.org/10.1136/bjophthalmol-2022-321295..

8. Yoshihara N, Yamashita T, Ohno-Matsui K, Sakamoto T. Objective analyses of tessellated fundi and significant correlation between degree of tessellation and choroidal thickness in healthy eyes. PLoS One. 2014;9(7):e103586.

9. Pan Y, Liu J, Cai Y, et al. Fundus image classification using inception v3 and resnet-50 for the early diagnostics of fundus diseases. Front Physiol. 2023;14:1126780.

10. Shao L, Zhang QL, Long TF, et al. Quantitative assessment of fundus tessellated density and associated factors in fundus images using artificial intelligence. Transl Vis Sci Technol. 2021;10(9):23.

11. Runkuan L, Xiaoxiao G, Zhang X, et al. Application of artificial intelligence to quantitative assessment of fundus tessellated density in young adults with different refractions. Ophthalmic Res 2023. https://doi.org/10.1159/000529639.

12. Shao L, Zhang X, Hu T, et al. Prediction of the fundus tessellation severity with machine learning methods. Front Med (Lausanne). 2022;9: 817114.

13. Zhao X, Li R, Huang D, et al. Decreased retinal thickness in preschool offspring of maternal gestational hypertension: the nanjing eye study. Acta Ophthalmol. 2020;98(6):e674–9.

14. Wang Z, Huang D, Chen X, et al. Preschool children exhibit evident compensatory role of internal astigmatism in distribution of astigmatism: the nanjing eye study. Invest Ophthalmol Vis Sci. 2019;60(1):73–81.

15. Xu Y, Ling SG, Dong Z, et al. development and application of a fundus image quality assessment system based on computer vision technology. Zhonghua Yan Ke Za Zhi. 2020;56(12):920–7.

16. Xu Y, Wang Y, Liu B, et al. The diagnostic accuracy of an intelligent and automated fundus disease image assessment system with lesion quantitative function (Smarteye) in diabetic patients. BMC Ophthalmol. 2019;19(1):184.

17. Terasaki H, Yamashita T, Yoshihara N, et al. Location of tessellations in ocular fundus and their associations with optic disc tilt, optic disc area, and axial length in young healthy eyes. PLoS One. 2016;11(6): e0156842.

18. Xiao O, Guo X, Wang D, et al. Distribution and severity of myopic maculopathy among highly myopic eyes. Invest Ophthalmol Vis Sci. 2018;59(12):4880–5.

19. Cheng T, Deng J, Xu X, et al. Prevalence of fundus tessellation and its associated factors in chinese children and adolescents with high myopia. Acta Ophthalmol. 2021;99(8):e1524–33.

20. Lyu H, Chen Q, Hu G, et al. Characteristics of fundal changes in fundus tessellation in young adults. Front Med (Lausanne). 2021;8: 616249.

21. Yamashita T, Iwase A, Kii Y, et al. Location of ocular tessellations in Japanese: population-based kumejima study. Invest Ophthalmol Vis Sci. 2018;59(12): 4963–7.

22. Yan YN, Wang YX, Yang Y, et al. Ten-year progression of myopic maculopathy: the Beijing Eye Study 2001–2011. Ophthalmology. 2018;125(8): 1253–63.

23. Wang R, He J, Chen Q, et al. Efficacy of a deep learning system for screening myopic maculopathy based on color fundus photographs. Ophthalmol Ther. 2023;12(1):469–84.

24. He X, Zou H, Lu L, et al. Axial length/corneal radius ratio: association with refractive state and role on myopia detection combined with visual acuity in chinese schoolchildren. PLoS One. 2015;10(2): e0111766.

25. Foo VH, Verkicharla PK, Ikram MK, et al. Axial length/corneal radius of curvature ratio and myopia in 3-year-old children. Transl Vis Sci Technol. 2016;5(1):5.